ELECTRONIC RESEARCH ARCHIVE
Volume **28**, Number **4**, December **2020**

doi:10.3934/era.2020076
pp. **1439–1457**

A ROBUST ADAPTIVE GRID METHOD FOR SINGULARLY PERTURBED BURGER-HUXLEY EQUATIONS

Li-Bin Liu*, Ying Liang and Jian Zhang

School of Mathematics and Statistics
Nanning Normal University
Nanning 530001, China

Xiaobing Bao

School of Big Data and Artificial Intelligence
Chizhou University
Chizhou, Anhui 247000, China

Abstract. In this paper, an adaptive grid method is proposed to solve one-dimensional unsteady singularly perturbed Burger-Huxley equation with appropriate initial and boundary conditions. Firstly, we use the classical backward-Euler scheme on a uniform mesh to approximate time derivative. The resulting nonlinear singularly perturbed semi-discrete problem is linearized by using Newton-Raphson-Kantorovich approximation method which is quadratically convergent. Then, an upwind finite difference scheme on an adaptive nonuniform grid is used for space derivative. The nonuniform grid is generated by equidistribution of a positive monitor function, which is similar to the arc-length function. It is shown that the presented adaptive grid method is first order uniform convergent in the time and spatial directions, respectively. Finally, numerical results are given to validate the theoretical results.

1. Introduction.

In this paper, we consider the following one-dimensional unsteady singularly perturbed Burger-Huxley equation

$$\begin{cases} \mathcal{L}_{x,\varepsilon} u(x,t) \equiv -\varepsilon \dfrac{\partial^2 u}{\partial x^2} + \alpha u \dfrac{\partial u}{\partial x} + \dfrac{\partial u}{\partial t} - \beta(1-u)(u-\gamma)u = 0, \\ (x,t) \in \Omega \times (0,T] \equiv (0,1) \times (0,T], \\ u(x,0) = u_0(x),\ x \in \overline{\Omega} = [0,1], \\ u(0,t) = S_0(t),\ u(1,t) = S_1(t),\ t \in (0,T], \end{cases} \tag{1}$$

where $0 < \varepsilon \ll 1$ is a perturbation parameter and $\alpha,\ \beta \geq 0,\ \gamma \in (0,1)$ are given constants. Such equation describes the interaction between convection, diffusion and reaction.

2020 *Mathematics Subject Classification.* 65M06, 65M12, 65M50.

Key words and phrases. Singularly perturbed, Burger-Huxley equation, upwind finite difference scheme, adaptive grid, uniform convergent.

The first author is supported by National Science Foundation of China (11761015), the Natural Science Foundation of Guangxi(2020GXNSFAA159010), the key project of Natural Science Foundation of Guangxi(2017GXNSFDA198014, 2018GXNSFDA050014), the key project of Natural Science Foundation of Chizhou University(CZ2018ZR06).

* Corresponding author: liulibin969@163.com.

It is well known that the Burger-Huxley equation describes many phenomena such as busting oscillation[9], interspike[24], population genetics[1], bifurcation and chaos[33]. In the past few decades, various analytical methods were proposed to solve the Burger-Huxley equation. For instance, by using Hirota method, Satsuma [30] obtained an exact solitary solution for this equation. Wang *et.al.*, [31] constructed an exact solitary wave solution of the generalized Burger-Huxley equation. In[32], Wazwaz derived some travelling wave solutions for the generalized forms of Burgers, Burgers-KdV and Burger-Huxley equation by using the standard tanh-function technique. Recently, many researches paid attention to solve Burger-Huxley equation by the numerical methods such as a domian decomposition method[15, 14, 16], variational iteration method[2], finite difference scheme[27, 28], spectral methods[8, 17, 18], collocation method[26, 20, 25]. However, for suitable values of α, β, γ and $0 < \varepsilon \ll 1$, the solution of Burger-Huxley problem, which is called singularly perturbed Burger-Huxley problem, usually has one or two boundary layers. Due to the presence of boundary layer(s), the above presented methods are in question and known to be inadequate to approximate the exact solution. Therefore, to obtain ε-uniformly convergent methods, Kaushik and Sharma[19] developed a parameter-uniform convergent finite difference scheme for the problem (1). Gupta and Kadalbajoo[13] constructed a numerical scheme that comprises of implicit-Euler method which is first order uniformly accurate to discretize in temporal direction on a uniform mesh and a monotone hybrid finite difference operator to discretize the spatial variable with a piecewise uniform Shishkin mesh. For the spatial direction, their method has been shown to be first order parameter uniform convergent in the outside region of boundary layer, and almost second order parameter uniform convergent in the boundary layer region.

Obviously, the methods presented in [19, 13] are belong to the lay-adapted mesh approach. As far as we know, the convergence results for the layer-adapted mesh approach is more easy to be obtained. But this special mesh approach requires a priori information about the location and width of the boundary layer. So, it is very necessary to study the adaptive moving grid approach by equidistributing a positive monitor function. Since this method has an advantage that it can be applied using little or no a priori information.

In order to serve this purpose, we will devise a uniformly convergent numerical scheme for the problem (1). We first use the classical backward-Euler formula on a uniform mesh to approximate the time derivative. The resulting nonlinear singularly perturbed ordinary differential equation is linearized by using quasi-lineariztion technique. Then, an upwind finite difference scheme is used for space discretization. The a posteriori error bound is derived to design an adaptive spatial grid generation algorithm. Finally, the convergence analysis is given to show that the presented adaptive grid method is first-order in the time and spatial directions, respectively.

2. **Bounds on the solution and its time derivatives.** In this section, we will give error estimates for the solution of continuous problem and its time derivatives. Let $D = (0,1) \times (0,T]$, the initial boundary $\Gamma_i = \{(x,t) : t = 0, x \in [0,1]\}$, left boundary $\Gamma_l = \{(x,t) : x = 0, t \in [0,T]\}$ and right boundary $\Gamma_r = \{(x,t) : x = 1, t \in [0,T]\}$, then, $\partial D = \Gamma_l \bigcup \Gamma_i \bigcup \Gamma_r$. For any given function $g(x,t) \in C^0(\overline{D})$, the maximum norm is defined as follows

$$\|g(x,t)\|_{\overline{D}} = \max_{(x,t)\in\overline{D}} |g(x,t)|.$$

First, the operator $\mathcal{L}_{x,\varepsilon}$ defined in (1) satisfies the following maximum principle.

Lemma 2.1. *(Maximum principle) Let $v(x,t) \in C^{2,1}(\overline{D})$. If $v(x,t) \geq 0$, $\forall(x,t) \in \partial D$ and $\mathcal{L}_{x,\varepsilon} v(x,t) \geq 0$, $\forall(x,t) \in D$, then $v(x,t) \geq 0$, $\forall(x,t) \in \overline{D}$.*

Proof. The proof can be seen in Lemma 1 of [13]. □

Furthermore, based on the above maximum principle, the following lemma [13] gives the uniform stability estimate.

Lemma 2.2. *Let $u(x,t)$ be the solution of the problem (1), then we have*

$$\|u\|_{\overline{D}} \leq T\|u_0\|_{\Gamma_i} + \|u\|_{\partial D}.$$

Finally, to derive the convergence and stability of the time discrete scheme, we give the bounds on the time derivatives as follows:

Lemma 2.3. *Let $u(x,t)$ be the solution of the problem (1). Then there exists a constant C, independent of ε, such that*

$$\left|\frac{\partial^i u(x,t)}{\partial t^i}\right| \leq C,\ i = 0, 1, 2,\ \forall(x,t) \in [0,1] \times (0,T].$$

Proof. It follows from Lemma 2.2, we can obtain $|u(x,t)| \leq C$. Next, one can obtain the first-order derivative bound with respect to time variable as follows.

First, at $t = 0$, we have $u(x,0) = u_0(x)$, which gives $\frac{\partial u(x,0)}{\partial x} = u_0'(x)$ and $\frac{\partial^2 u(x,0)}{\partial x^2} = u_0''(x)$, $x \in [0,1]$. Then, we get

$$\begin{aligned}\frac{\partial u(x,0)}{\partial t} = \varepsilon \frac{\partial^2 u(x,0)}{\partial x^2} - \alpha u(x,0)\frac{\partial u(x,0)}{\partial x}& \\ + \beta(1-u(x,0))(u(x,0)-\gamma)u(x,0),\ x \in [0,1].&\end{aligned}$$

On the boundaries $x = 0$ and $x = 1$, we obtain

$$\frac{\partial u(0,t)}{\partial t} = S_0'(t),\ \frac{\partial u(1,t)}{\partial t} = S_1'(t),\ t \in (0,T].$$

Therefore, for sufficiently smooth functions $u_0(x)$, $S_0(t)$ and $S_1(t)$, there exists a constant C_1, such that

$$\left|\frac{\partial u(x,t)}{\partial t}\right| \leq C_1,\ \forall(x,t) \in \partial D.$$

For $\forall(x,t) \in (0,1) \times (0,T]$, it follows from (1) that

$$\mathcal{L}_{x,\varepsilon}\frac{\partial u(x,t)}{\partial t} = 0.$$

As the operator $\mathcal{L}_{x,\varepsilon}$ is uniformly stable, using Lemma 2.2, we get

$$\left|\frac{\partial u(x,t)}{\partial t}\right| \leq C,\ (x,t) \in \overline{D}.$$

Similarly, we get the bound for the second-order derivative $\frac{\partial^2 u(x,t)}{\partial t^2}$. □

3. **Time semi-discretization and quasi-linearization.**

3.1. **Time semi-discretization.** Let

$$S_t^M = \{t_n = n\Delta t, n = 0, \cdots, M, \Delta t = T/M\}$$

be a uniform mesh in time direction, where M denotes the number of mesh intervals in the time direction. Here, discretizing the problem (1) with respect to temporal variable by using the backward Euler method, we can obtain the following non-linear ordinary differential equations

$$\begin{cases} u^0 = u(x,0) = u_0(x), x \in \overline{\Omega}, \\ (I + \Delta t \bar{\mathcal{L}}_{x,\varepsilon})u^{n+1} \equiv -\varepsilon \Delta t \dfrac{\partial^2 u^{n+1}}{\partial x^2} + \alpha \Delta t u^{n+1} \dfrac{\partial u^{n+1}}{\partial x} \\ \qquad\qquad - \beta \Delta t (1 - u^{n+1})(u^{n+1} - \gamma) u^{n+1} + u^{n+1} = u^n, \\ u^{n+1}(0) = S_0(t^{n+1}),\ u^{n+1}(1) = S_1(t^{n+1}), \end{cases} \tag{2}$$

where u^n is the semi-discrete approximation to the exact solution $u(x,t)$ of the continuous problem (1) at time level $t_n = n\Delta t$, $0 \le n \le M-1$.

Next, to analyze the uniform convergence of the solution u^n to the exact solution $u(x,t_n)$, we will do the stability analysis and derive the consistency result of the scheme (2). Obviously, the operator $(I + \Delta t \bar{\mathcal{L}}_{x,\varepsilon})$ satisfies the maximum principle, which ensures the stability of the scheme (2).

Let $e_{n+1} = u(x, t_{n+1}) - \widehat{u}^{n+1}(x)$ be the local error of semi-discretization scheme (2), where $\widehat{u}^{n+1}(x)$ is the solution obtained after one step of semi-discrete scheme (2) by taking the exact value $u(x,t_n)$ instead of $u^n(x)$ as the starting data. Then, we obtain the following boundary value problem

$$\begin{cases} \widehat{u}^{n+1}(x) + \Delta t \bar{\mathcal{L}}_{x,\varepsilon} \widehat{u}^{n+1}(x) = u^n,\ x \in (0,1),\ n \ge 0, \\ u^{n+1}(0) = S_0(t^{n+1}),\ u^{n+1}(1) = S_1(t^{n+1}),\ n \ge 0. \end{cases} \tag{3}$$

Lemma 3.1. *Let e_{n+1} be the local error of semi-discretization scheme (2), then, we have*

$$\|e_{n+1}\|_\infty \le C(\Delta t)^2. \tag{4}$$

Proof. Since the solution of the problem (1) is smooth enough, by using Taylor series expansion, we have

$$\begin{aligned} u^n &= u^{n+1} - \Delta t \frac{\partial u^{n+1}}{\partial t} + \int_{t^n}^{t^{n+1}} (t^n - s) \frac{\partial^2 u(x,s)}{\partial t^2} ds \\ &= u^{n+1} - \Delta t \left\{ \varepsilon \frac{\partial^2 u^{n+1}}{\partial x^2} - \alpha u^{n+1} \frac{\partial u^{n+1}}{\partial x} + \beta (1 - u^{n+1})(u^{n+1} - \gamma) u^{n+1} \right\} \\ &\quad + \frac{\partial^2 u(x,\xi)}{\partial t^2} O((\Delta t)^2), \end{aligned}$$

where $\xi \in (t^n, t^{n+1})$.

Then by applying Taylor expansion to linearize the nonlinear differential operator $\bar{\mathcal{L}}_{x,\varepsilon}$, the desired estimate (4) follows from Lemma 1 of [7]. □

Based on the above results, we can obtain the following global error estimate.

Theorem 3.2.

$$\sup_{n \le T/\Delta t} \|u(x,t_n) - u^n(x)\|_\infty \le C\Delta t. \tag{5}$$

Thus, the semi-discretization (2) is uniformly convergent of first-order in time.

3.2. **Quasilinearization.** In this section, we will introduce the Newtom-Raphson-Kantorovich approximation approach to linearize the nonlinear differential equation (2). For the nonlinear ordinary differential equation $u'' = f(u, u', x)$, Bellman and Kalaba[3] developed the following linearization scheme

$$\begin{aligned} u''_{(k+1)} =& f(u_{(k)}, u'_{(k)}, x) + (u_{(k+1)} - u_{(k)}) f_u(u_{(k)}, u'_{(k)}, x) \\ &+ (u'_{(k+1)} - u'_{(k)}) f_{u'}(u_{(k)}, u'_{(k)}, x), \end{aligned} \tag{6}$$

where $\{u_{(k)}\}_{k=0}^{\infty}$ are a sequence of approximate solutions of $u'' = f(u, u', x)$.

Here, in our case, based on the scheme (6), the time semi-discretisation (2) can be written as

$$u^0_{(k+1)} = u_0(x),\ x \in [0,1], \tag{7}$$

$$\begin{aligned} &-\varepsilon \Delta t \frac{\partial^2 u^{n+1}_{(k+1)}}{\partial x^2} + \alpha \Delta t u^{n+1}_{(k)} \frac{\partial u^{n+1}_{(k+1)}}{\partial x} + \Bigg(\alpha \Delta t u^{n+1}_{(k)} \frac{\partial u^{n+1}_{(k)}}{\partial x} + \beta \Delta t ((u^{n+1}_{(k)} - \gamma) \\ &-(1 - u^{n+1}_{(k)}) - (1 - u^{n+1}_{(k)})(u^{n+1}_{(k)} - \gamma)) \Bigg) = u^n_{(k+1)} + \alpha \Delta t u^{n+1}_{(k)} \frac{\partial u^{n+1}_{(k)}}{\partial x} \\ &+\beta \Delta t \left((1 - u^{n+1}_{(k)})(u^{n+1}_{(k)} - \gamma) u^{n+1}_{(k)} + (u^{n+1}_{(k)} - \gamma) u^{n+1}_{(k)} \right. \\ &\left. -(1 - u^{n+1}_{(k)}) u^{n+1}_{(k)} - (1 - u^{n+1}_{(k)})(u^{n+1}_{(k)} - \gamma) \right),\ x \in [0,1],\ n \geq 0, \end{aligned} \tag{8}$$

with the boundary conditions

$$u^{n+1}_{(k+1)}(0) = S_0(t^{n+1}),\ u^{n+1}_{(k+1)}(1) = S_1(t^{n+1}),\ n \geq 0, \tag{9}$$

where $u_{(k)}$ is the nominal solution of the problem (2) with a reasonable initial guess $u_{(0)}$ satisfying the initial condition $u_0(x)$ and $k = 0, 1, 2, \cdots$, is the iteration index.

For the sake of convenience, let $u_{(k+1)} = \widetilde{u}$, the above equation can be written as

$$\widetilde{u}^0 = u_0(x),\ x \in [0,1], \tag{10}$$

$$\begin{aligned} (I + \Delta t \widetilde{\mathcal{L}}_{x,\varepsilon}) \widetilde{u}^{n+1} \equiv& -\varepsilon \Delta t \frac{\partial^2 \widetilde{u}^{n+1}}{\partial x^2} + a^{n+1}(x) \Delta t \frac{\partial \widetilde{u}^{n+1}}{\partial x} \\ &+ (1 + \Delta t b^{n+1}(x)) \widetilde{u}^{n+1} = \widetilde{u}^n + \Delta t f^{n+1}(x),\ x \in [0,1],\ n \geq 0, \end{aligned} \tag{11}$$

$$\widetilde{u}^{n+1}(0) = S_0(t^{n+1}),\ \widetilde{u}^{n+1}(1) = S_1(t^{n+1}),\ n \geq 0, \tag{12}$$

where

$$\begin{aligned} a^{n+1}(x) &= a_{(k)}(x, t^{n+1}) = \alpha u^{n+1}_{(k)}, \\ b^{n+1}(x) &= b_{(k)}(x, t^{n+1}) = \alpha \frac{\partial u^{n+1}_{(k)}}{\partial x} + \beta \left(-2u^{n+1}_{(k)} + 3 \left[u^{n+1}_{(k)} \right]^2 + \gamma - 2\gamma u^{n+1}_{(k)} \right), \\ f^{n+1}(x) &= f_{(k)}(x, t^{n+1}) = \alpha u^{n+1}_{(k)} \frac{\partial u^{n+1}_{(k)}}{\partial x} + \beta \left(2 \left[u^{n+1}_{(k)} \right]^3 - (1 + \gamma) \left[u^{n+1}_{(k)} \right]^2 \right). \end{aligned}$$

Here, for $n \geq 0$, assuming that $a^{n+1}(x)$, $b^{n+1}(x)$ and $f^{n+1}(x)$ are sufficiently smooth functions and there exist two positive constants p and q such that

$$a^{n+1}(x) \geq p > 0,\ b^{n+1}(x) \geq q > 0,\ \ \forall x \in [0,1],\ n \geq 0.$$

Under these conditions, the solution of above problem (10)-(12) has a unique solution that usually has a boundary layer at $x = 1$ for $\varepsilon \to 0$, see, e.g.,[29]. For

$k = 0, 1, 2, \cdots$ and $n \geq 0$, we will solve the sequence of second order singularly perturbed linear boundary value problem (10)-(12) instead of solving the original nonlinear problem (2). Furthermore, for the solution $u^{n+1}(x)$ of original nonlinear problem (2), we should prove that

$$\lim_{k\to+\infty} u_{(k)}^{n+1}(x) = u^{n+1}(x),\ x \in [0,1], \tag{13}$$

whereas numerically, we require that

$$\left|\widetilde{u}^{n+1}(x) - u_{(k)}^{n+1}(x)\right| < \varepsilon,\ \ x \in [0,1], \tag{14}$$

where ε is a small tolerance value to terminate the computation.

Now, to obtain (13) or (14), the following theorem shows that not only the convergence of this sequence $\left\{u_{(k)}^{n+1}\right\}_{k=0}^{\infty}$ is quadratic, but also its proportionality constant is independent of k.

Theorem 3.3. *Let $\left\{u_{(k)}^{n+1}\right\}_{k=0}^{\infty}$ be the sequence produced by quasilinearization technique at $(n+1)$ time level. Then, there exists a positive constant C, independent of k, such that*

$$\|u_{(k+1)}^{n+1} - u_{(k)}^{n+1}\|_\infty \leq C\|u_{(k)}^{n+1} - u_{(k-1)}^{n+1}\|_\infty^2.$$

Proof. The proof can be seen in Theorem 5 of [13]. □

4. **Spatial discretization.** In this section, we shall develop a finite difference scheme of (10)-(12) on the following non-uniform spatial mesh

$$\overline{\Omega}_x^N = \{0 = x_0 < x_1 < \cdots < x_N = 1\}.$$

Here, the spatial step size is denoted by

$$h_i = x_i - x_{i-1},\ i = 1, \cdots, N.$$

Firstly, for a given mesh function $v(x_i, t_n) = v_i^n$, we define some difference operators as follows:

$$D_x^+ v_i^n = \frac{v_{i+1}^n - v_i^n}{h_{i+1}},\ D_x^- v_i^n = \frac{v_i^n - v_{i-1}^n}{h_i},$$
$$D_x^2 v_i^n = \frac{D_x^+ v_i^n - D_x^- v_i^n}{\hbar_i},\ \hbar_i^n = \frac{h_i + h_{i+1}}{2}.$$

Then, on $\overline{\Omega}_x^N$, the finite difference spatial discretization of (10)-(12) takes the form

$$\begin{cases} U_i^0 = u_0(x_i), \\ (I + \Delta t \bar{\mathcal{L}}_{x,\varepsilon}^N) U_i^{n+1} = U_i^n + \Delta t f_i^{n+1},\ i = 1, \cdots, N-1, n \geq 0, \\ U_0^{n+1} = S_0(t^{n+1}),\ U_N^{n+1} = S_1(t^{n+1}),\ n \geq 0, \end{cases} \tag{15}$$

where $\bar{\mathcal{L}}_{x,\varepsilon}^N$ is the discretization of the differential operator $\bar{\mathcal{L}}_{x,\varepsilon}$, which takes the following form:

$$\bar{\mathcal{L}}_{x,\varepsilon}^N U_i^{n+1} = -\varepsilon D_x^2 U_i^{n+1} + a_i^{n+1} D_x^- U_i^{n+1} + b_i^{n+1} U_i^{n+1}.$$

Here, U_i^n is the numerical solution of exact solution $u(x_i, t_n)$ and

$$a_i^{n+1} = a(x_i, t^{n+1}),\ b_i^{n+1} = b(x_i, t^{n+1}),\ f_i^{n+1} = f(x_i, t^{n+1}).$$

Remark 1. Here, by choosing a reasonable initial approximation $u_{(0)}^{n+1}$, we iteratively solve the linear boundary value problem (10)-(12) to obtain the solution $u_{(k)}^{n+1}$. At every iteration, we opt to numerically solve the problem (10)-(12) using the upwind finite difference scheme (15), where we use the center finite difference scheme to approximate the derivatives $\frac{\partial u_{(k)}^{n+1}}{\partial x}$ given in $b^{n+1}(x)$ and $f^{n+1}(x)$.

5. **Adaptive spatial grid algorithm.** It is well known that the monitor functions are used by many authors [21, 22, 4, 5] to obtain adaptive grid algorithms that produce layer-resolving meshes in solving singularly perturbed ordinary differential equations. In recent years, there has been tremendous interest in developing the adaptive grid approach of singularly perturbed parabolic equations [10, 11, 12]. It should be pointed out that the authors in [10, 11] obtained a different spatial mesh on each time level t_n by equidistributing a monitor function $M(u(x,t_n),x)$. Meanwhile, the authors[12] used the idea of equidistributing the spatial grids for a fixed time level $T_0(0 < T_0 \leq T)$ and obtained a spatial grid for all the levels. However, it is hard to find the fixed time level T_0 which can reflect the information of boundary layer. This drawback motivates to construct a spatial grid which is suitable for all time levels, in which the same order of convergence and the error estimation can be established.

Here, for singularly perturbed Burger-Huxley equation, in order to construct such a nonuniform spatial grid, we use the idea of equidistribution of a monitor function which is given by

$$M(u(x,t),x) = \max_{0\leq t\leq T}\left\{\sqrt{1+\left|\frac{\partial u(x,t)}{\partial x}\right|^2}\right\}. \tag{16}$$

Thus, a grid is said to be equidistributing $M(u(x,t),x)$, if

$$\int_{x_{i-1}}^{x_i} M(u(s,t),s)ds = \frac{1}{N}\int_0^1 M(u(s,t),s)ds,\ i=1,\cdots,N. \tag{17}$$

Let $\widehat{U}^n(x) \in C[0,1]$ be a piecewise linear interpolant function through the knots (x_i, U_i^n). Then, in practical computation, we choose the following monitor function

$$\widetilde{M}(u(x,t),x) = \max_{0\leq n\leq T/\Delta t}\left\{\sqrt{1+\left|\left(\widehat{U}^n(x)\right)'\right|^2}\right\}, \tag{18}$$

which is the discrete analogue of the monitor function (16).

Therefore, to obtain the equidistribution grid and the corresponding numerical solution, we construct the following iteration algorithm:

Step 1. Take $k=0$, let the uniform spatial mesh $\left\{x_i^{(k)} = i/N, i=0,1,\cdots,N\right\}$ be the initial mesh.

Step 2. For $k=1,2,\cdots$, assuming that the mesh $\left\{x_i^{(k)}\right\}$ is given, compute the discrete solution $U_i^{n,(k)}$ that satisfy (15) on $\left\{x_i^{(k)}\right\}$. For each i, let $h_i^{(k)} = x_i^{(k)} - x_{i-1}^{(k)}$ and

$$l_i^{(k)} = h_i^{(k)} \max_{0\leq n\leq T/\Delta t}\left\{\sqrt{1+\left(D_x^- U_i^{n,(k)}\right)^2}\right\}$$

$$= \max_{0\le n\le T/\Delta t}\left\{\sqrt{\left(h_i^{(k)}\right)^2+\left(U_i^{n,(k)}-U_{i-1}^{n,(k)}\right)^2}\right\}$$

be the maximum distance between the points $\left(x_{i-1}^{(k)},U_{i-1}^{n,(k)}\right)$ and $\left(x_i^{(k)},U_i^{n,(k)}\right)$. Then, the total maximum arc-length can be written as

$$L^{(k)}=\sum_{i=1}^{N} l_i^{(k)}=\sum_{i=1}^{N}\max_{0\le n\le T/\Delta t}\left\{\sqrt{\left(h_i^{(k)}\right)^2+\left(U_i^{n,(k)}-U_{i-1}^{n,(k)}\right)^2}\right\}.$$

Step 3. Test mesh: Let C_0 be a user chosen constant with $C_0>1$. If the stopping criterion

$$\frac{\max\limits_{1\le i\le N} l_i^{(k)}}{L^{(k)}}\le\frac{C_0}{N} \tag{19}$$

holds true, then go to **Step 5**. Otherwise, continue to **Step 4**.

Step 4. Generate a new mesh by equidistributing arc-length of current computed solution: choose point $0=x_0^{(k+1)}<x_1^{(k+1)}<\cdots<x_N^{(k+1)}=1$ such that

$$\int_{x_{i-1}^{(k+1)}}^{x_i^{(k+1)}}\sqrt{1+\max_{0\le n\le T/\Delta t}\left\{\widehat{U}^{n,(k)}(x)\right\}}=L^{(k)}/N,$$

where $i=1,2,\cdots,N$ and $\widehat{U}^{n,(k)}(x)\in C[0,1]$ is a piecewise linear interpolant function through the knots $\left(x_i,U_i^{n,(k)}\right)$. Return to **Step 3**.

Step 5. Take $\left\{x_i^{(k)}\right\}$ as the final mesh and calculate the corresponding solution U_i^n, then stop.

6. **Error analysis.** In this section, in order to derive an a posteriori error estimate for the fully discrete scheme of (15), we will list some preliminary results as follows.

Firstly, we rewrite (11) in the form

$$\widetilde{\mathcal{L}}_{x,\varepsilon}\widetilde{u}^{n+1}=-\frac{\widetilde{u}^{n+1}-\widetilde{u}^{n}}{\Delta t}+f^{n+1}(x)\equiv g^n(x)+\phi^{n+1}(x),\ x\in(0,1), \tag{20}$$

$$\widetilde{u}^{n+1}(0)=S_0(t^{n+1}),\ \widetilde{u}^{n+1}(1)=S_1(t^{n+1}), \tag{21}$$

where $\phi^{n+1}(x)=f^{n+1}(x)=f_{(k)}(x,t^{n+1})$, $n\ge 0$.

It is easy to see that the operator $(I+\Delta t\widetilde{\mathcal{L}}_{x,\varepsilon})$ satisfies the maximum principle, which implies $\left\|\widetilde{u}^{n+1}\right\|_\infty\le C$. In addition, under the sufficient smoothness of the function $f^{n+1}(x)$, the function $g^n(x)+f^{n+1}(x)$ is ε-uniformly bounded in the spatial domain.

Denote

$$\begin{aligned}
&\widetilde{\mathbf{u}}=(\widetilde{u}^1,\widetilde{u}^2,\cdots,\widetilde{u}^M)^T,\\
&\mathbf{S}_0=(S_0(t^1),\cdots,S_0(t^M))^T,\\
&\mathbf{S}_1=(S_1(t^1),\cdots,S_1(t^M))^T,\\
&\mathbf{F}(x)=(g^0(x)+\phi^1(x),\cdots,g^{M-1}(x)+\phi^M(x))^T,
\end{aligned}$$

the Equation (20) can be written into the following system of equations

$$\widetilde{\mathcal{L}}_{x,\varepsilon}\widetilde{\mathbf{u}}\equiv-\varepsilon\widetilde{\mathbf{u}}_{xx}+A(x)\widetilde{\mathbf{u}}_x+B(x)\widetilde{\mathbf{u}}=\mathbf{F}(x),\ x\in(0,1), \tag{22}$$

$$\widetilde{\mathbf{u}}(0)=\mathbf{S}_0,\ \widetilde{\mathbf{u}}(1)=\mathbf{S}_1, \tag{23}$$

where $A(x) = \mathrm{diag}(a^1(x), \cdots, a^M(x))$, $B(x) = \mathrm{diag}(b^1(x), \cdots, b^M(x))$ are $M \times M$ diagonal matrixes, respectively.

Obviously, the simple upwind finite difference scheme of (22) can be written into the following matrix form

$$\mathcal{L}_{x,\varepsilon}^N \widetilde{\mathbf{U}}_i \equiv -\varepsilon D_x^2 \widetilde{\mathbf{U}}_i + A(x_i) D_x^- \widetilde{\mathbf{U}}_i + B(x_i)\widetilde{\mathbf{U}}_i = \mathbf{F}(x_i), \tag{24}$$

$$\widetilde{\mathbf{U}}(0) = \mathbf{S}_0,\ \widetilde{\mathbf{U}}(1) = \mathbf{S}_1, \tag{25}$$

where $\widetilde{\mathbf{U}}_i = (\widetilde{U}_i^1, \cdots, \widetilde{U}_i^M)^T$ is the approximation solution of $\widetilde{\mathbf{u}}(x_i)$.

Next, based on the above preparation work, we can obtain the following result:

Theorem 6.1. *Let $\widetilde{\mathbf{u}}(x)$ be the solution of (22), $\widetilde{\mathbf{U}}_i$ be the solution of (24) on an arbitrary nonuniform mesh $\overline{\Omega}_x^N$ and $\widehat{\mathbf{U}}(x)$ be piecewise linear interpolant function vector through knots $(x_i, \widetilde{\mathbf{U}}_i)$. Then we have*

$$\|\widetilde{\mathbf{u}}(x) - \widehat{\mathbf{U}}(x)\|_\infty \le C \left\{ \max_{1\le i\le N} h_i \left[\max_{1\le n\le M} \left| D_x^- \widetilde{U}_i^n \right| \right] + \max_{1\le i\le N} h_i \right\}. \tag{26}$$

Proof. The proof is similar to Theorem 3.1 in [23]. □

Furthermore, based on the properties of discrete Green's function[22], we can obtain the following convergence result:

Theorem 6.2. *Let $\widetilde{\mathbf{u}}(x)$ be the solution of (22), $\widetilde{\mathbf{U}}_i$ be the solution of (24) on a nonuniform grid $\{x_i\}_{i=0}^N$ generated by the above adaptive spatial grid algorithm. Then we have the following bound*

$$\left\| \widetilde{\mathbf{u}}(x_i) - \widetilde{\mathbf{U}}_i \right\|_\infty \le CN^{-1}. \tag{27}$$

Proof. The proof is similar to Theorem 4.2 in [6]. □

From Theorem 6.2, an easy induction gives the following result:

Theorem 6.3. *For each time level $n = 1, \cdots, M$, let $\widetilde{u}^n(x)$ be the solution of problem (10)-(12) and $\widetilde{U}_i^n$ be the solution of discrete system (24) calculated on a grid $\{x_i\}_{i=0}^N$ generated by the above adaptive spatial grid algorithm. Then we have the following bound*

$$\max_{0\le i\le N} \left| \widetilde{u}^n(x_i) - \widetilde{U}_i^n \right| \le CN^{-1}. \tag{28}$$

Corollary 1. *If we take $N^{-q} \le C\Delta t$ with $0 < q < 1$, then we have*

$$\max_{0\le i\le N} \left| \widetilde{u}^n(x_i) - \widetilde{U}_i^n \right| \le C\Delta t N^{-1+q}. \tag{29}$$

Now, we give the main result of our paper.

Theorem 6.4. *Let $u(x,t)$ be the exact solution of the Burgers-Huxley equation (1), $\widetilde{u}^n(x)$ be the solution of the semi-discrete problem (10)-(12) after the time discretization and quasilinearization process and U_i^n be the solution of fully discrete scheme (15) calculated on a grid $\{x_i\}_{i=0}^N$ generated by the above adaptive spatial grid algorithm and time level $t_n = n\Delta t$. Assume that $N^{-q} \le C\Delta t$ with $0 < q < 1$. Then we have the following bound*

$$\max_{0\le i\le N} |u(x_i, t_n) - U_i^n| \le C(\Delta t + N^{-1+q}). \tag{30}$$

Proof. Let $E_i^n = u(x_i, t_n) - U_i^n$, $0 \le i \le N$ be the global error at time level t_n, $1 \le n \le M$. Then, splitting the global error $\{E_i^n\}$ as follows:

$$|E_i^n| \le |u(x_i, t_n) - \widehat{u}^n(x_i)| + |\widehat{u}^n(x_i) - \widetilde{u}^n(x_i)| + |\widetilde{u}^n(x_i) - \widetilde{U}_i^n| + |\widetilde{U}_i^n - U_i^n|.$$

From (4) and Corollary 1, we have

$$\max_{0 \le i \le N} |u(x_i, t_n) - \widehat{u}^n(x_i)| \le C (\Delta t)^2, \tag{31}$$

$$\max_{0 \le i \le N} \left| \widetilde{u}^n(x_i) - \widetilde{U}_i^n \right| \le C \Delta t N^{-1+q}. \tag{32}$$

For $\forall \varepsilon > 0$, it follows from Theorem 3.3 that

$$|\widehat{u}^n(x_i) - \widetilde{u}^n(x_i)| < \varepsilon. \tag{33}$$

Then, by applying the stability of the fully discrete scheme (15), we obtain

$$\max_{0 \le i \le N} \left| \widetilde{U}_i^n - U_i^n \right| \le C \max_{0 \le i \le N} \left| u(x_i, t_{n-1}) - U_i^{n-1} \right|. \tag{34}$$

Finally, let $\varepsilon = C\Delta t(\Delta t + N^{-1+q}) > 0$, from (31)-(34), we obtain the following recurrence relation:

$$\max_{0 \le i \le N} |E_i^n| \le C\Delta t(\Delta t + N^{-1+q}) + \max_{0 \le i \le N} \left| E_i^{n-1} \right|, \tag{35}$$

and hence, the result (30) follows from it. □

7. **Numerical examples and discussion.** In this section, we will give some numerical results obtained by the fully discrete scheme (15) for two test problems on the rectangular mesh $\overline{\Omega}_x^N \times S_t^M$, where $\overline{\Omega}_x^N$ is the equidistribution mesh generated from the numerical algorithm. It is well known that the constant C_0 in the above adaptive spatial mesh algorithm gives an intimation of how close we are from the equidistribution of the monitor function. In all the numerical experiments, we take $C_0 = 2$ and begin with $N = 32$ and the time step $\Delta t = 0.05$ and we multiply N by two and divide Δt by two.

For small enough values of the parameters ε, the exact solution of the following examples are not available. Therefore, we use the double mesh principal to calculate the maximum point-wise error, which are defined as

$$E_\varepsilon^{N,M} = \max_{\substack{0 \le i \le N, \\ 0 \le n \le M}} \left| U^{N,M}(x_i, t_n) - U^{2N,2M}(x_i, t_n) \right|, \tag{36}$$

where $U^{N,M}(x_i, t_n)$ denote the numerical solution obtained on the mesh with N mesh intervals in the spatial direction and M mesh intervals in the time direction. From these values, we compute the corresponding order of convergence by

$$r_\varepsilon^{N,M} = \log_2 \left(\frac{E_\varepsilon^{N,M}}{E_\varepsilon^{2N,2M}} \right). \tag{37}$$

In addition, for the above Newton linearization process, we use the following convergence criterion for the numerical solution

$$\left| U_{(k+1)}^{n+1}(x_i) - U_{(k)}^{n+1}(x_i) \right| \le 10^{-10}.$$

Here, we chose 0 as the initial guess in all cases and the iterations were stopped when the absolute error tolerance is achieved.

For comparison purposes, we use the upwind differences scheme (15) on the piecewise-uniform Shishkin mesh, which is constructed as follows[19, 13]: Let N

be divisible by 2 and τ be the transition parameter which determines the point of transition from a fine mesh to the coarse mesh and is defined as

$$\tau = \min\left[\frac{1}{2}, \theta\varepsilon \ln N\right], \tag{38}$$

where θ is the constant whose value depends upon the method applied. Here, we choose $\theta = 1$. Then, we divide $[0,1]$ into two subdomains $[0, 1-\tau]$ and $[1-\tau, 1]$. Finally, we place $N/2$ number of subintervals in each of the subdomains and obtain the Shishkin mesh as follows:

$$\overline{\Omega}_\varepsilon^N = \left\{x_i : x_i = 2\tau i/N, 0 \le i \le N/2; x_i = x_{i-1} + 2(1-\tau)/N, N/2 < i \le N\right\}.$$

Example 5.1. In this example, we consider the following singularly perturbed Burgers-Huxley equation

$$\begin{cases} \dfrac{\partial u}{\partial t} + u\dfrac{\partial u}{\partial x} - \varepsilon\dfrac{\partial^2 u}{\partial x^2} - (1-u)(u-0.5)u = 0, \ (x,t) \in (0,1)\times(0,1], \\ u(x,0) = x(1-x^2), \ 0 < x < 1, \\ u(0,t) = u(1,t) = 0, \ t \in [0,1]. \end{cases} \tag{39}$$

In Table 1, we give the maximum point-wise error $E_\varepsilon^{N,M}$ for $\varepsilon = 2^{-j}$, $j = 0, 2, \cdots, 18$. Meanwhile, the orders of convergence associated with the fully discrete scheme (15) are listed in Table 2. It is shown from these results that, with the increase of N and M, the convergence order of the presented numerical method is more and more close to 1. To compare our results, the computed errors and the corresponding orders of convergence for the well-known layer-adapted meshes, Shishkin mesh, are given in Tables 3-4. Obviously, as can be seen from Tables 1-4 that adaptive grid method presented in this paper produced better results than that produced by using the Shishkin mesh.

In addition, the numerical solution is plotted in Figure 1 for $N = 64$, $M = 40$ and $\varepsilon = 2^{-14}$. Meanwhile, Figure 2 shows the computed solution at different time levels. It is shown from Figures 1-2 that the numerical solution of Example 5.1 has a boundary layer near $x = 1$ with the time variable $t \to 1$. Furthermore, in order to make the reader's understanding of the meshes generation by the above spatial grid algorithm, the process of grid movement after each iteration is plotted in Figure 3 for $N = 64$, $M = 40$ and $\varepsilon = 2^{-12}$, which should be read from bottom to top. The left of this figure is labeled with the value of C_0 for which the stopping criterion (19) becomes an equation. It is shown from Figure 3 that taking any smaller value of C_0 will increase the number of iterations. Obviously, the mesh starts to move toward the boundary $x = 1$ after each iteration. Thus, the presented adaptive grid method has the advantage that without any prior information of the boundary layer.

Example 5.2. Consider the following singularly perturbed Burger's equation:

$$\begin{cases} u_t + u\dfrac{\partial u}{\partial x} - \varepsilon u_{xx} = 0, \ (x,t) \in (0,1)\times(0,1], \\ u(x,0) = x(1-x^2), \ 0 < x < 1, \\ u(0,t) = u(1,t) = 0, \ t \in [0,1]. \end{cases} \tag{40}$$

For $\varepsilon = 2^{-j}$, $j = 0, 2, \cdots, 18$, the calculated maximum point-wise errors and the corresponding order convergence for Example 5.2 are listed in Tables 5-6, respectively. The numerical results given in Table 6 reveal the first-order uniform convergence with the increase of N and M. Furthermore, we have also compared

TABLE 1. Maximum error of solution $E_\varepsilon^{N,M}$ for Example 5.1 using the adaptive grid method.

ε	Number of intervals N/time size Δt					
	$32/\frac{1}{20}$	$64/\frac{1}{40}$	$128/\frac{1}{80}$	$256/\frac{1}{160}$	$512/\frac{1}{320}$	$1024/\frac{1}{640}$
2^0	2.4400e-02	1.4033e-02	7.5889e-03	3.9547e-03	2.0227e-03	1.0233e-03
2^{-2}	1.8830e-02	1.1126e-02	6.5407e-03	3.6221e-03	1.9209e-03	1.0074e-03
2^{-4}	2.0658e-02	1.2614e-02	7.0567e-03	3.7952e-03	1.9563e-03	1.0231e-03
2^{-6}	2.5289e-02	1.7672e-02	9.0066e-03	4.8378e-03	2.5035e-03	1.2731e-03
2^{-8}	3.8607e-02	1.9497e-02	1.1221e-02	6.2852e-03	3.3405e-03	1.7233e-03
2^{-10}	9.3183e-02	7.0120e-02	4.4773e-02	2.0546e-02	1.0545e-02	5.1608e-03
2^{-12}	1.7017e-01	1.0083e-01	6.2216e-02	3.9526e-02	2.0493e-02	1.0027e-02
2^{-14}	2.0410e-01	1.6703e-01	9.2110e-02	5.2580e-02	2.8766e-02	1.6523e-02
2^{-16}	2.0450e-01	1.5975e-01	1.2612e-01	6.9772e-02	3.8531e-02	2.0526e-02
2^{-18}	2.5614e-01	2.1031e-01	1.3406e-01	8.5618e-02	4.8834e-02	2.6219e-02

TABLE 2. Rate of convergence of solution $r_\varepsilon^{N,M}$ for Example 5.1 using the adaptive grid method.

ε	Number of intervals N/time size Δt				
	$32/\frac{1}{20}$	$64/\frac{1}{40}$	$128/\frac{1}{80}$	$256/\frac{1}{160}$	$512/\frac{1}{320}$
2^0	0.7981	0.8869	0.9403	0.9673	0.9831
2^{-2}	0.7591	0.7664	0.8526	0.9150	0.9311
2^{-4}	0.7117	0.8380	0.8948	0.9560	0.9352
2^{-6}	0.5170	0.9724	0.8966	0.9504	0.9756
2^{-8}	0.9856	0.7971	0.8362	0.9119	0.9549
2^{-10}	0.4102	0.6472	1.1238	0.9623	1.0309
2^{-12}	0.7550	0.6966	0.6544	0.9477	1.0312
2^{-14}	0.2892	0.8587	0.8088	0.8701	0.7999
2^{-16}	0.3563	0.3410	0.8540	0.8566	0.9086
2^{-18}	0.2844	0.6496	0.6469	0.8100	0.8973

TABLE 3. Maximum error of solution $E_\varepsilon^{N,M}$ for Example 5.1 calculated on Shishkin grid.

ε	Number of intervals N/time size Δt					
	$32/\frac{1}{20}$	$64/\frac{1}{40}$	$128/\frac{1}{80}$	$256/\frac{1}{160}$	$512/\frac{1}{320}$	$1024/\frac{1}{640}$
2^0	2.5632e-02	1.6476e-02	9.9288e-03	5.6712e-03	3.1149e-03	1.7000e-03
2^{-2}	2.9611e-02	1.8504e-02	1.0796e-02	6.0104e-03	3.2417e-03	1.7105e-03
2^{-4}	3.1540e-02	2.0968e-02	1.1706e-02	6.3027e-03	3.3320e-03	1.7024e-03
2^{-6}	3.4637e-02	1.7587e-02	7.9159e-03	3.8469e-03	2.2367e-03	2.5185e-03
2^{-8}	8.3069e-02	6.3873e-02	3.7579e-02	1.9554e-02	9.7037e-03	3.0087e-03
2^{-10}	8.3319e-02	1.1804e-01	8.7025e-02	5.1153e-02	2.7435e-02	1.1428e-02
2^{-12}	5.9149e-02	1.2245e-01	1.4419e-01	9.5806e-02	5.5767e-02	2.7152e-02
2^{-14}	3.8012e-02	1.2070e-01	1.9830e-01	1.4945e-01	9.1763e-02	5.4821e-02
2^{-16}	3.7835e-02	8.8086e-02	1.9473e-01	2.0775e-01	1.3885e-01	9.6989e-02
2^{-18}	3.7788e-02	3.6581e-02	1.7951e-01	2.5413e-01	1.9134e-01	1.4338e-01

TABLE 4. Rate of convergence of solution $r_\varepsilon^{N,M}$ for Example 5.1 calculated on Shishkin grid.

ε	Number of intervals N/time size Δt				
	$32/\frac{1}{20}$	$64/\frac{1}{40}$	$128/\frac{1}{80}$	$256/\frac{1}{160}$	$512/\frac{1}{320}$
2^0	0.6375	0.7307	0.8079	0.8644	0.8736
2^{-2}	0.6783	0.7773	0.8450	0.8907	0.9223
2^{-4}	0.5890	0.8409	0.8932	0.9196	0.9688
2^{-6}	0.9778	1.1517	1.0411	0.7823	-0.1712
2^{-8}	0.3791	0.7653	0.9425	1.0108	1.6893
2^{-10}	-0.5026	0.4398	0.7666	0.8988	1.2634
2^{-12}	-1.0498	-0.2357	0.5897	0.7807	1.0384
2^{-14}	-1.6666	-0.7162	0.4080	0.7037	0.7432
2^{-16}	-1.2192	-1.1445	-0.0933	0.5814	0.5176
2^{-18}	0.0468	-2.2948	-0.5015	0.4093	0.4163

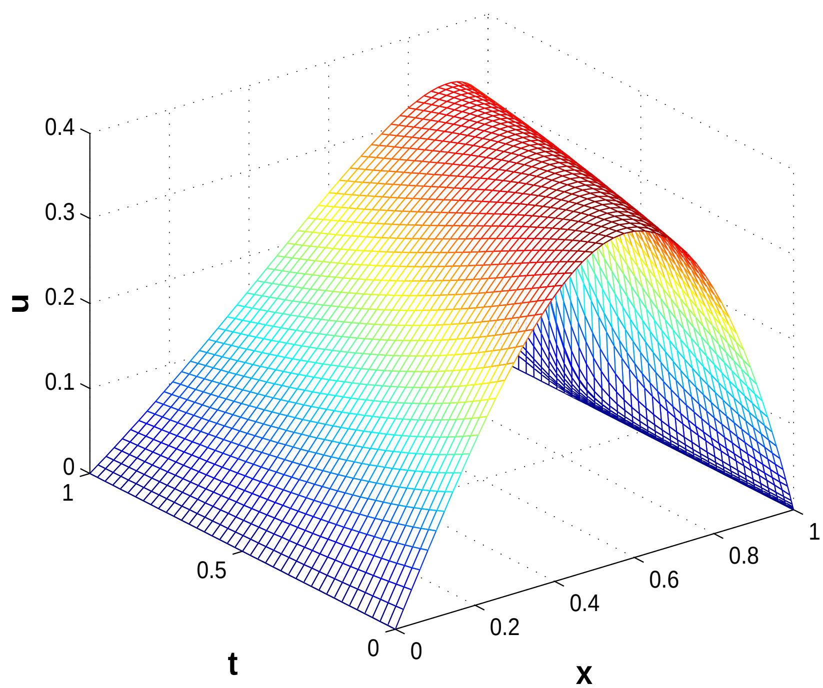

FIGURE 1. Numerical solution profile of Example 5.1 with $N = 64$, $M = 40$ and $\varepsilon = 2^{-14}$.

the numerical results using the presented method to that using the Shishkin mesh, see Tables 7-8. It is shown from Tables 5-8 that the presented adaptive grid method is better than the Shishkin mesh method. Figure 4 displays the numerical solution of Example 5.2 at different time levels. Figure 5 shows the mesh movement after

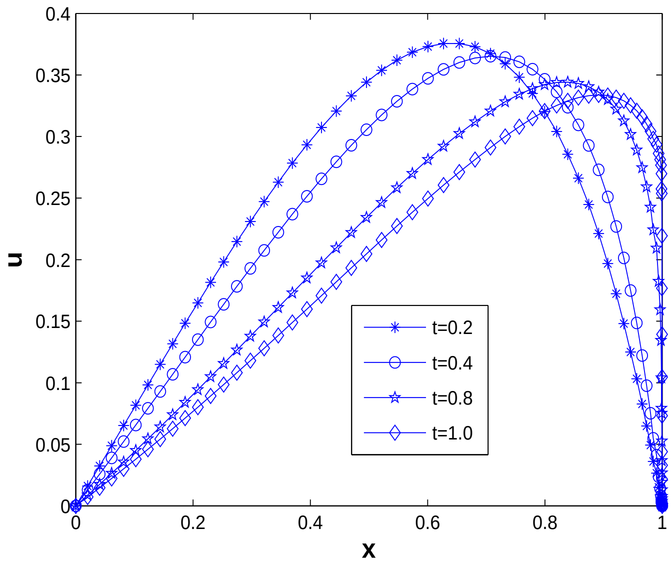

FIGURE 2. Numerical solution of Example 5.1 at different time levels with $N = 64$, $M = 40$ and $\varepsilon = 2^{-14}$.

each iteration. These figures also show the existence of the boundary layer at $x = 1$ with time variable $t \to 1$.

8. **Conclution.** The present paper discusses a parameter-uniform numerical method for the singularly perturbed Burgers-Huxley equation. At first, for discretizing the time derivative, we use the classical backward-Euler method and for the spatial discretization the simple upwind scheme is used on a nonuniform grid. An iterative method based on Newton-Raphson-Kantorovich technique is presented

TABLE 5. Maximum error of solution $E_\varepsilon^{N,M}$ for Example 5.2 using the adaptive grid method.

ε	Number of intervals N/time size Δt					
	$32/\frac{1}{20}$	$64/\frac{1}{40}$	$128/\frac{1}{80}$	$256/\frac{1}{160}$	$512/\frac{1}{320}$	$1024/\frac{1}{640}$
2^{0}	2.4502e-02	1.4057e-02	7.5969e-03	3.9589e-03	2.0249e-03	1.0244e-03
2^{-2}	1.9156e-02	1.1404e-02	6.5847e-03	3.6356e-03	1.9226e-03	1.0085e-03
2^{-4}	2.2788e-02	1.3365e-02	7.2769e-03	3.8441e-03	1.9728e-03	1.0270e-03
2^{-6}	3.8767e-02	1.8983e-02	9.6122e-03	5.0867e-03	2.6211e-03	1.3306e-03
2^{-8}	4.4450e-02	2.0109e-02	1.0519e-02	5.9653e-02	3.1896e-03	1.6508e-03
2^{-10}	8.3339e-02	6.6120e-02	4.0769e-02	1.9284e-02	9.1775e-03	4.9998e-03
2^{-12}	1.8762e-01	8.4106e-02	5.7234e-02	3.8309e-02	1.9041e-02	9.2260e-03
2^{-14}	1.9755e-01	1.5347e-01	8.3864e-02	4.6945e-02	2.5508e-02	1.4930e-02
2^{-16}	2.1340e-01	1.5016e-01	1.1582e-01	6.1958e-02	3.3441e-02	1.7672e-02
2^{-18}	2.8299e-01	1.7036e-01	1.1805e-01	7.4251e-02	4.1879e-02	2.2413e-02

TABLE 6. Rate of convergence of solution $r_\varepsilon^{N,M}$ for Example 5.2 using the adaptive grid method.

ε	Number of intervals N/time size Δt				
	$32/\frac{1}{20}$	$64/\frac{1}{40}$	$128/\frac{1}{80}$	$256/\frac{1}{160}$	$512/\frac{1}{320}$
2^{0}	0.8016	0.8878	0.9403	0.9672	1.1059
2^{-2}	0.7843	0.7924	0.8864	0.9191	0.9308
2^{-4}	0.7698	0.8771	0.9207	0.9624	0.9418
2^{-6}	1.0301	0.9818	0.9181	0.9566	0.9781
2^{-8}	1.1443	0.9348	0.8183	0.9032	0.9502
2^{-10}	0.3339	0.6976	1.0801	1.0712	0.8762
2^{-12}	1.1575	0.5553	0.5792	1.0086	1.0453
2^{-14}	0.3643	0.8718	0.8371	0.8800	0.7727
2^{-16}	0.5076	0.3746	0.9025	0.8897	0.9202
2^{-18}	0.7322	0.5292	0.6689	0.8262	0.9019

TABLE 7. Maximum error of solution $E_\varepsilon^{N,M}$ for Example 5.2 calculated on Shishkin grid.

ε	Number of intervals N/time size Δt					
	$32/\frac{1}{20}$	$64/\frac{1}{40}$	$128/\frac{1}{80}$	$256/\frac{1}{160}$	$512/\frac{1}{320}$	$1024/\frac{1}{640}$
2^{0}	2.4502e-02	1.4057e-02	7.5969e-03	3.9589e-03	2.0249e-03	1.6649e-03
2^{-2}	3.0271e-02	1.8725e-02	1.0868e-02	6.0332e-03	3.2486e-03	1.7125e-03
2^{-4}	3.7645e-02	2.2072e-02	1.2090e-02	6.4115e-03	3.3584e-03	1.7453e-03
2^{-6}	3.6325e-02	2.6153e-02	1.6509e-02	9.7972e-03	5.6201e-03	2.9364e-03
2^{-8}	9.9532e-02	5.4894e-02	2.7274e-02	1.2963e-02	6.0337e-03	3.6346e-03
2^{-10}	2.1833e-01	1.5551e-01	8.7820e-02	4.5033e-02	2.2291e-02	1.3620e-02
2^{-12}	2.2602e-01	2.6665e-01	1.8203e-01	1.0258e-01	5.2694e-02	2.9881e-02
2^{-14}	1.2823e-01	3.2914e-01	2.7178e-01	1.8208e-01	1.0356e-01	5.2147e-02
2^{-16}	4.4024e-02	3.2475e-01	3.2607e-01	2.5174e-01	1.6644e-01	8.0344e-02
2^{-18}	3.3007e-02	2.5627e-01	3.5442e-01	2.9823e-01	2.1963e-01	1.2277e-01

TABLE 8. Rate of convergence of solution $r_\varepsilon^{N,M}$ for Example 5.2 calculated on Shishkin grid.

ε	Number of intervals N/time size Δt				
	$32/\frac{1}{20}$	$64/\frac{1}{40}$	$128/\frac{1}{80}$	$256/\frac{1}{160}$	$512/\frac{1}{320}$
2^{-0}	0.8016	0.8878	0.9403	0.9672	0.2824
2^{-2}	0.6930	0.7849	0.8491	0.8931	0.9237
2^{-4}	0.7702	0.8684	0.9151	0.9329	0.9443
2^{-6}	0.4740	0.6637	0.7528	0.8018	0.9365
2^{-8}	0.8585	1.0091	1.0731	1.1033	0.7312
2^{-10}	0.4895	0.8244	0.9636	1.0145	0.7107
2^{-12}	-0.2385	0.5508	0.8274	0.9610	0.8184
2^{-14}	-1.3600	0.2763	0.5779	0.8141	0.9898
2^{-16}	-2.8830	-0.0059	0.3732	0.5969	1.0507
2^{-18}	-2.9568	-0.4678	0.2490	0.4388	0.8391

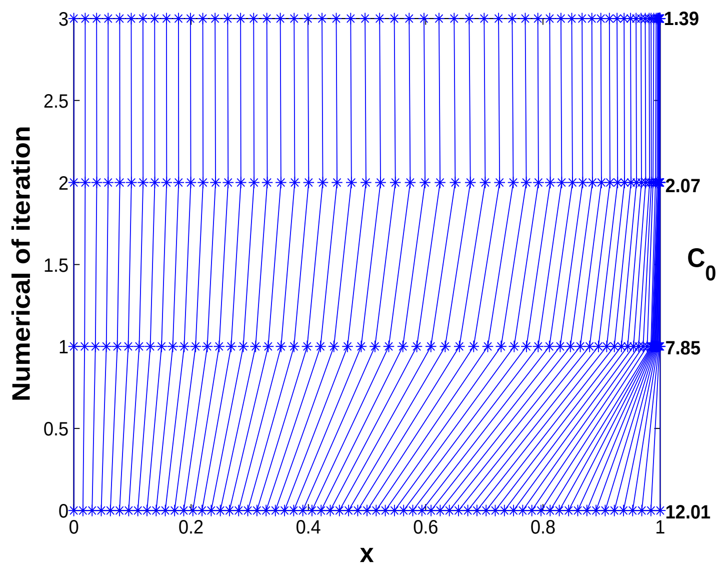

Figure 3. Mesh movement of Example 5.1 for $N = 64$, $M = 40$ and $\varepsilon = 2^{-12}$.

to process the nonlinear term of the Burgers-Huxley equation. Parameter-uniform error estimations are derived for the numerical solution. It is also shown from the numerical results that the proposed numerical method has a better numerical accuracy compared to the Shishkin grid method. In all, for the numerical methods of the singularly perturbed Burgers-Huxley equation, the adaptive grid method is very effective.

REFERENCES

[1] D. G. Aronson and H. F. Weinberger, Multidimensional nonlinear diffusion arising in population genetics, *Adv. Math.*, **30** (1978), 33–76.

[2] B. Batiha, M. S. M. Noorani and I. Hashim, Numerical simulation of the generalized Huxley equation by He's variational iteration method, *Appl. Math. Comput.*, **186** (2007), 1322–1325.

[3] R. E. Bellman and R. E. Kalaba, *Quasilineaization and Nonlinear Boundary-Value Problems*, Modern Analytic and Computional Methods in Science and Mathematics, Vol. 3 American Elsevier Publishing Co., Inc., New York 1965.

[4] Y. Chen, Uniform pointwise convergence for a singularly perturbed problem using arc-length equidistribution, *J. Comput. Appl. Math.*, **159** (2003), 25–34.

[5] Y. Chen, Uniform convergence analysis of finite difference approximations for singular perturbation problems on an adapted grid, *Adv. Comput. Math.*, **24** (2006), 197–212.

[6] Y. Chen, L.-B. Liu, An adaptive grid method for singularly perturbed time-dependent convection-diffusion problems, *Commum. Comput. Phys.*, **20** (2016), 1340–1358.

[7] C. Clavero, J. C. Jorge and F. Lisbona, A uniformly convergent scheme on a nonuniform mesh for convection–diffusion parabolic problems, *J. Comput. Appl. Math.*, **154** (2003), 415–429.

[8] M. T. Darvishi, S. Kheybari and F. Khani, Spectral collocation method and Darvishi's preconditionings to solve the generalized Burgers-Huxley equation, *Commun. Nonlinear Sci. Numer. Simul.*, **13** (2008), 2091–2103.

[9] L. Duan and Q. Lu, Bursting oscillations near codimension-two bifurcations in the Chay neuron model, *Int. J. Nonlinear Sci. Numer. Simul.*, **7** (2006), 59–63.

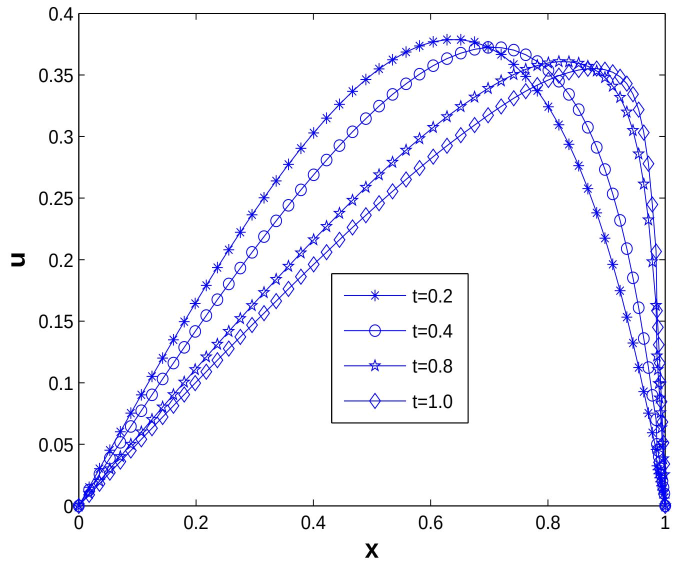

FIGURE 4. Numerical solution of Example 5.2 at different time levels with $N = 64$, $M = 40$ and $\varepsilon = 2^{-8}$.

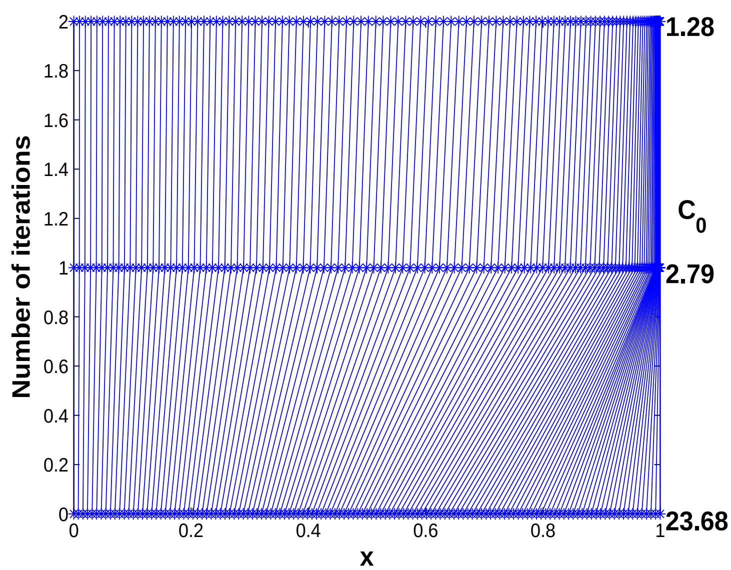

FIGURE 5. Mesh movement of Example 5.2 for $N = 128$, $M = 80$ and $\varepsilon = 2^{-10}$.

[10] S. Gowrisankar and S. Natesan, The parameter uniform numerical method for singularly perturbed parabolic reaction-diffusion problems on equidistributed grids, *Appl. Math. Lett.*, **26** (2013), 1053–1060.

[11] S. Gowrisankar and S. Natesan, Uniformly convergent numerical method for singularly perturbed parabolic initial-boundary-value problems with equidistributed grids, *Int. J. Comput. Math.*, **91** (2014), 553–577.

[12] S. Gowrisankar and S. Natesan, Robust numerical scheme for singularly perturbed convection-diffusion parabolic initial-boundary-value problems on equidistributed grids, *Comput. Phys. Commun.*, **185** (2014), 2008–2019.

[13] V. Gupta and M. K. Kadalbajoo, A singular perturbation approach to solve Burgers-Huxley equation via monotone finite difference scheme on layer-adaptive mesh, *Commun. Nonlinear Sci. Numer. Simul.*, **16** (2011), 1825–1844.

[14] I. Hashim, M. S. M. Noorani and B. Batiha, A note on the Adomian decomposition method for the generalized Huxley equation, *Appl. Math. Comput.*, **181** (2006), 1439–1445.

[15] I. Hashim, M. S. M. Noorani and M. R. Said Al-Hadidi, Solving the generalized Burgers-Huxley equation using the adomian decomposition method, *Math. Comput. Model.*, **43** (2006), 1404–1411.

[16] H. N. A. Ismail, K. Raslan and A. A. A. Rabboh, Adomian decomposition method for Burgers-Huxley and Burgers-Fisher equations, *Appl. Math. Comput.*, **159** (2004), 291–301.

[17] M. Javidi, A numerical solution of the generalized Burgers-Huxley equation by spectral collocation method, *Appl. Math. Comput.*, **178** (2006), 338–344.

[18] M. Javidi and A. Golbabai, A new domain decomposition algorithm for generalized Burgers-Huxley equation based on Chebyshev polynomials and preconditioning, *Chaos Solitons Fractals*, **39** (2009), 849–857.

[19] A. Kaushik and M. D. Sharma, A uniformly convergent numerical method on non-uniform mesh for singularly perturbed unsteady Burger-Huxley equation, *Appl. Math. Comput.*, **195** (2008), 688–706.

[20] A. J. Khattak, A computational meshless method for the generalized Burger's-Huxley equation, *Appl. Math. Model.*, **33** (2009), 3718–3729.

[21] N. Kopteva, Maximum norm a posteriori error estimates for a one-dimensional convection-diffusion problem, *SIAM J. Numer. Anal.*, **39** (2001), 423–441.

[22] N. Kopteva and M. Stynes, A robust adaptive method for quasi-linear one-dimensional convection-diffusion problem, *SIAM J. Numer. Anal.*, **39** (2001), 1446–1467.

[23] L.-B. Liu and Y. Chen, A robust adaptive grid method for a system of two singularly perturbed convection-diffusion equations with weak coupling, *J. Sci. Comput.*, **61** (2014), 1–16.

[24] S. Liu, T. Fan and Q. Lu, The spike order of the winnerless competition (WLC) model and its application to the inhibition neural system, *Int. J. Nonlin. Sci. Numer. Simul.*, **6** (2005), 133–138.

[25] R. C. Mittal and A. Tripathi, Numerical solutions of generalized Burgers-Fisher and generalized Burgers-Huxley equations using collocation of cubic B-splines, *Int. J. Comput. Math.*, **92** (2015), 1053–1077.

[26] R. Mohammadi, B-spline collocation algorithm for numerical solution of the generalized Burger's-Huxley equation, *Numer. Methods Partial Differential Equations*, **29** (2013), 1173–1191.

[27] R. K. Mohanty, W. Dai and D. Liu, Operator compact method of accuracy two in time and four in space for the solution of time dependent Burgers-Huxley equation, *Numer. Algorithms*, **70** (2015), 591–605.

[28] S. Murat, G. Görhan and Z. Asuman, High-order finite difference schemes for numerical solutions of the generalized Burgers-Huxley equation, *Numer. Methods Partial Differential Equations*, **27** (2011), 1313–1326.

[29] H.-G. Roos, M. Stynes and L. Tobiska, *Numerical Methods for Singularly Perturbed Differential Equations*, Convection-diffusion and flow problems. Springer Series in Computational Mathematics, 24. Springer-Verlag, Berlin, 1996.

[30] J. Satsuma J, *Topics in Soliton Theory and Exactly Solvable Nonlinear Equations*, World Scientific, Singapore, 1987.

[31] X. Y. Wang, Z. S. Zhu and Y. K. Lu, Solitary wave solutions of the generalised Burgers-Huxley equation, *J. Phys. A*, **23** (1990), 271–274.

[32] A.-M. Wazwaz, Travelling wave solutions of generalized forms of Burgers, Burgers-KdV and Burgers-Huxley equations, *Appl. Math. Comput.*, **169** (2005), 639–656.

[33] G.-J. Zhang, J.-X. Xu, H. Yao et al., Mechanism of bifurcation-dependent coherence resonance of an excitable neuron model, *Int. J. Nonlin. Sci. Numer. Simul.*, **7** (2006), 447–450.

Received November 2019; revised July 2020.

E-mail address: liulibin969@163.com
E-mail address: l_ying321@163.com
E-mail address: 546552279@qq.com
E-mail address: czubxb@163.com